RSC Advances

PAPER

View Article Online
View Journal | View Issue

Cite this: *RSC Adv.*, 2025, **15**, 49545

pH-Responsive polymeric vesicles prepared *via* polymerization-induced self-assembly for controlled 5-fluorouracil delivery

Laila M. Alhaidari, *[a] Reema Altariqi,[a] Thana Alkhamis,[a] Reem Alanezi[a] and Nada M. Merghani[b]

Received 24th August 2025
Accepted 2nd December 2025

DOI: 10.1039/d5ra06313b

rsc.li/rsc-advances

Stimuli-responsive polymeric vesicles are promising nanocarriers for the controlled release of chemotherapeutic agents. Although pH-responsive poly(2-(diisopropylamino)ethyl methacrylate) (PDPA) vesicles have been widely studied for the delivery of drugs such as doxorubicin hydrochloride, their use in 5-fluorouracil (5-FU) delivery has not been reported. Here, we demonstrate for the first time the application of PDPA-based vesicles for pH-triggered release of 5-FU. The vesicles were prepared *via* polymerization-induced self-assembly (PISA) using reversible addition–fragmentation chain transfer (RAFT) polymerization of DPA with poly(*N*,*N*-dimethylacrylamide) (PDMA) as a macro-chain transfer agent in a water/ethanol medium. The vesicles remained stable at physiological pH but disassembled under acidic conditions due to the hydrophobic-to-hydrophilic transition of the PDPA block, resulting in accelerated release of 5-FU. Cytotoxicity assays in HCT116 cells showed comparable anticancer efficacy between vesicle-loaded and free 5-FU, while blank vesicles were nontoxic. Confocal laser scanning microscopy (CLSM) confirmed efficient cellular uptake. These results highlight PDPA-based vesicles as a novel and effective nanoplatform for pH-responsive delivery of 5-FU.

Introduction

Polymerization-induced self-assembly (PISA) has presented itself as a versatile and straightforward technique for production of polymeric nanoparticles with diverse morphologies including spheres, worm-like, and vesicles. Unlike the traditional "solvent-switch" approach,[1,2] PISA allows the synthesis of nanoparticles in a single pot reaction at considerably greater concentrations (up to 50 wt%). PISA involves chain extension of a soluble polymer block, which acts as a stabilizer, with a monomer that produces a second insoluble polymer block to form the self-assembled amphiphilic nanoparticle *in situ*. PISA can be performed under either dispersion, in which the monomer is soluble, or emulsion polymerization mechanisms, in which the monomer is insoluble in the reaction medium. In principle, PISA can be mediated using any type of living/controlled polymerization, including anionic polymerization,[3,4] atom transfer radical polymerization (ATRP),[5,6] nitroxide mediated radical polymerization (NMP),[7] or reversible addition–fragmentation chain transfer (RAFT).[8,9] In practical, PISA is almost limited by RAFT[10–14] because of its applicability to polymerize various classes of functional monomers in a wide range of solvents.[15–17]

Among various polymeric morphologies, vesicles are especially attractive due to their unique morphology of amphiphilic polymeric bilayer membrane surrounding aqueous cores (lumen).[18,19] This unique morphology of vesicles allows the encapsulation of either hydrophilic or hydrophobic drug molecules (or both) within their aqueous cores and the hydrophobic membrane, respectively.[20] Compared to phospholipid bilayers in liposomes, polymeric vesicles membranes are thicker and more stable as a result of higher molar mass values of the block copolymers.[18] This in turn can substantially diminish the premature release of the encapsulated drugs during circulation and therefore reduce the cytotoxicity. More recently, intense interest has been devoted in the development of smart vesicles[21,22] that respond to certain stimuli, including pH,[23–27] temperature,[28,29] redox.[30,31] These vesicles are designed to be stable during circulation but release the loaded drugs rapidly in a controlled manner when the target site is reached. pH-responsive vesicles are particularly attractive because of the well-known acidic extracellular pH of solid tumor (6.8–7.2) in comparison with the physiological pH (7.4).[32] Furthermore, the pH value within lysosomes can be as low as 4.5.[33] Among various pH-responsive vesicles, polymeric vesicles bearing tertiary amino groups, including poly[2-(diisopropylamino)ethyl methacrylate] (PDPA), have particularly gain keen interest in drug delivery applications.[25,34,35] As a result of the reversible

[a]*Department of Chemistry, Faculty of Science, University of Majmaah, Majmaah, 11952, Saudi Arabia. E-mail: l.alhaidari@mu.edu.sa*

[b]*Central Research Laboratory, Vice Rectorate for Studies and Scientific Research, King Saud University, Riyadh, 12371, Saudi Arabia*

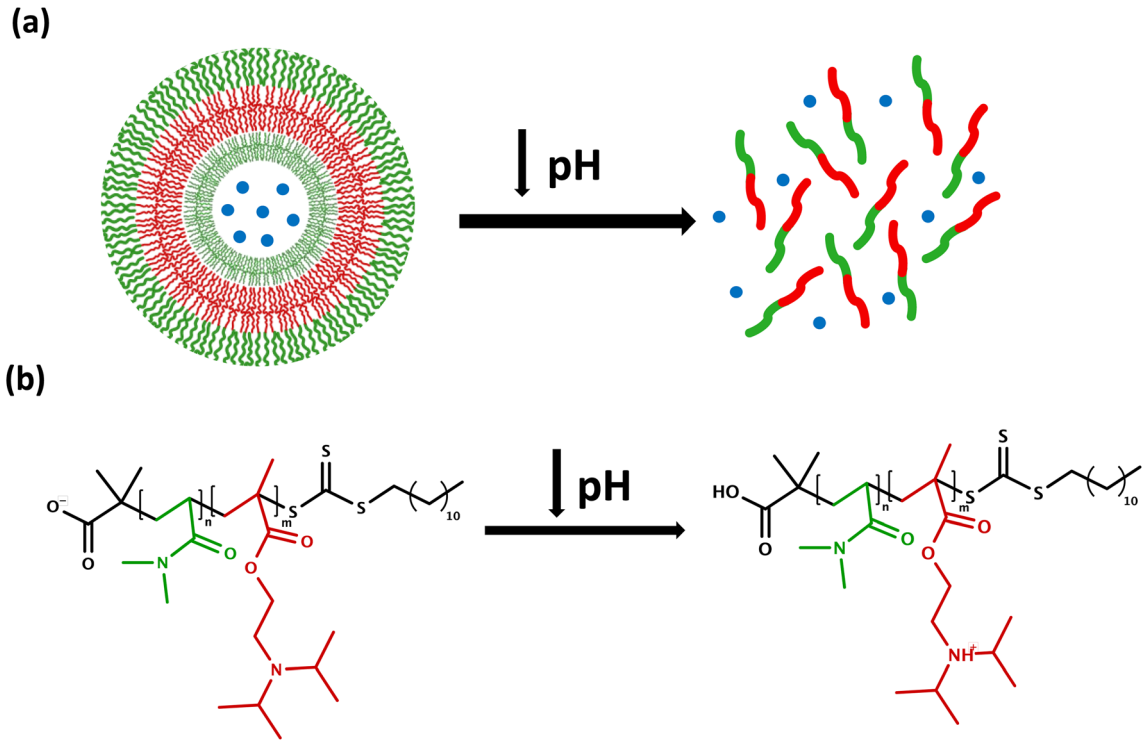

Fig. 1 (a) Block copolymer vesicles disassociation in response to change in pH (b) hydrophobic–hydrophilic transition of the tertiary amino group on PDPA block upon lowering pH value.

deprotonation and protonation of tertiary amino group, these polymeric vesicles can undergo either deswelling/swelling[26] or assembling/disassembling[25] transition upon a change in pH across pK_a ($\approx$6.3). Shape-persistent vesicles obtained by cross-linking of the membrane often undergo deswelling/swelling transition when the solution pH is lower than pK_a, whereas non-crosslinked vesicles disassemble to dissolved copolymer chains (unimer).

5-Fluorouracil (5-FU) is a hydrophilic chemotherapeutic agent that is commonly used against wide range of solid tumors, either alone or in combination with other drugs.[36] However, its clinical utility is severely limited by poor selectivity and systemic toxicity, often leading to adverse side effects. In an attempt to minimize its side effects and improve its therapeutic efficiency, a variety of drug delivery systems, in which 5-FU is conjugated[37–39] or encapsulated within vesicles,[40–42] have been developed. Despite the successful examples reported for 5-FU delivery, there is still a dearth of data on the development of smart carrier systems capable of providing triggered and site-specific release of 5-FU. Recently, several pH-responsive vesicles based on PDPA block have been synthesized and evaluated for the controlled release of hydrophilic chemotherapeutic agents (*e.g.*, DOX-HCl).[34,35] These systems exploit the reversible ionization of the tertiary amine groups in PDPA, which undergo a hydrophobic–hydrophilic transition under mildly acidic conditions, leading to vesicle disassembly and payload release. Building upon these advances, we hypothesized that PDPA-containing vesicles could provide an efficient and stimuli-responsive delivery platform for 5-FU. Herein, Herein, we report for the first time the design, synthesis, and evaluation of pH-responsive PDPA-containing vesicles for the controlled delivery of 5-FU. These vesicles were engineered to remain stable at physiological pH and undergo triggered disassembly under endosomal pH, enabling efficient 5-FU drug release (Fig. 1).

Experimental section

^{1}H NMR

Proton nuclear magnetic resonance (^{1}H NMR) spectra were recorded on Bruker AV800 spectrometer at room temperature. Deuterated chloroform ($CDCl_3$) and deuterium oxide (D_2O) were used as sample solvents. Chemical shifts of spectrums are estimated in ppm relative to TMS peak and the NMR spectra were examined using Topspin 4.3.0 NMR software.

DLS

Intensity-average size distributions were determined by Malvern Zetasizer software using a Malvern Zetasizer NanoZS Model ZEN 3600 instrument at a fixed angle of 173°. Measurements were performed at 25 °C on the polymer's solutions in distilled water with a concentration of 0.2 wt%. Three measurements of ten runs with ten seconds duration were made and averaged.

TEM

TEM studies were accomplished using Titan ST microscope operating at 300 kV (Thermofisher). Samples were prepared by placing a droplet (5 μL) of the polymer solution 0.2 wt% on Quatifoil grids (EMS) and set for air drying.

SEC

The molecular weight distribution of PDMA macro-CTA and PDMA$_n$-*co*-PDPA$_m$ diblock copolymers were determined by size exclusion chromatography (SEC) equipped with triple detector (only the refractive index detector was utilized). The SEC setup consisted of two 5 μm (7.5 × 300 mm) mixed C columns connected in series. The SEC eluent were either HPLC-grade THF or DMF at a flow rate of 1.0 mL min^{-1}. A series of ten near-monodisperse poly(methyl methacrylate) (PMMAs) standards (M_p values ranging from 1980 to 1 591 000 g mol^{-1}) were used for calibration. Data were analyzed using Agilent SEC software version 2.1.9.34851.

Materials

2-(Dodecylthiocarbonothioylthio)2-methylpropanoic acid (DDMAT) (Solarbio, ≥97%), 5-FU (Solarbio, ≥99%), *N*,*N*′-dimethylacetamide (DMAc) (Solarbio, ≥99%), 4-4′-azobis(4-cyanovaleric acid) (ACVA) (Solarbio, ≥98%), diethyl ether (Fisher, ≥99%), acetone (Fisher, ≥99%) Rhodamine B (Solarbio, ≥95%), and Hoechst Stain Solution (H6024, Sigma-Aldrich) were used as received. *N*,*N*-Dimethylacrylamide (DMA) (Solarbio, ≥99%), and 2-(diisopropylamino)ethyl methacrylate (DPA) (Sigma Aldrich, ≥97%) were passed through aluminum oxide to remove the inhibitor prior used. The human colon cell line (HCT116) was obtained from the American Type Culture Collection (ATCC, Rockville, MD, USA).

Synthesis of the PDMA as macro-CTA precursor by RAFT solution polymerization of DMA in DMAc

DMA (6 g, 30.30 mmol), ACVA (0.068 g, 0.1212 mmol) and DDMAT (0.44 g, 0.06 mmol) with ratio [50 : 1 : 0.2] were dissolved in (6.92 mL) of anhydrous DMAc and degassed by purging the reaction mixture with nitrogen for 45 min. The sealed Schlenk flask was immersed in a preheated water bath set at 60 °C with a stirring speed of 400 rpm for 2.5 h. Prior to purification, a sample of crude reaction mixture was taken to calculate the monomer conversion using ^{1}H NMR. The polymer was purified *via* precipitation three times in diethylether : acetone 9 : 1. The precipitate was dried under high vacuum at room temperature until constant weight to afford a dry yellow powder. An overall yield of 90% was obtained. M_n and $Đ$ were estimated *via* SEC using DMF as eluent and PMMA standards.

Synthesis of PDMA$_{50}$-*b*-PDPA$_m$ diblock copolymer vesicles *via* PISA

An example of PISA dispersion for the synthesis targeting PDMA$_{50}$-*b*-PDPA$_{200}$ is as follows: PDMA (3.798×10^{-2} mmole, 200 mg), DPA (7.597 mmole, 1.620 g), and ACVA (7.597×10^{-3}, 2 mg) were dissolved in 20 wt% of water : ethanol 4 : 6. The reaction solution was purged with nitrogen gas for 30 min to remove oxygen. Then, the sealed vial was immersed in a preheated water bath set at 70 °C under a stirring speed of 400 rpm for 4 h. The reaction was quenched by exposing the reaction mixture to air. A sample was taken for determination of monomer conversion prior purification. The polymer was purified by dialysis (MWCO, 3.5 kDa) against deionized water for 24, which was dried under high vacuum at room temperature for ^{1}H NMR analysis. The M_n and $Đ_M$ values were estimated *via* THF SEC using PMMA standards.

Encapsulation of 5-FU within the PDMA$_{50}$-*b*-PDPA$_{200}$ vesicles

The PDMA$_{50}$-*b*-PDPA$_{200}$ vesicles 20 wt% water : ethanol dispersion (2.278 mL) and 5-FU (12 mg) were stirred under a stirring speed of 400 rpm for 48 h at room temperature. The resultant mixture was dialyzed (MWCO, 3.5 kDa) against deionized water to remove the unloaded 5-FU. The deionized water was renewed every 1 h until UV of 5-FU outside the dialysis tube was negligible. The concentration of 5-FU was evaluated *via* UV-vis spectra according to the standard curve. The loading content (LC) and the loading efficiency (LE) of 5-FU was calculated according to the following equations.

$$\text{LC\%} = \frac{\text{Mass of the loaded 5-FU}}{\text{Mass of the nanoparticles}} \quad (1)$$

$$\text{LE\%} = \frac{\text{Mass of the loaded 5-FU}}{\text{Mass of 5-FU used for the encapsulation}} \quad (2)$$

5-FU release study at pH 7.4 and pH 4.5

The cumulative release of 5-FU was accomplished using dialysis in both phosphate buffer (0.1 M) at pH 7.4, and acetate buffer (0.1 M) at pH 4.5. 800 μL of 5-FU-loaded vesicles was transferred into a dialysis tube (MWCO, 3.5 kDa), and then immersed in 10 mL of buffer under stirring (400 rpm). At the predetermined intervals, 2 mL outside of the dialysis tube was taken and replaced with an equal volume of fresh medium. The release behavior of 5-FU was monitored using UV-vis at a wavelength of 285 nm against standard calibration curves.

Determination of cytotoxicity

Cytotoxicity studies were performed using the human colon cell line (HCT116). Initially, cells were seeded in 96-well plate at a density of 2×10^5 cells per well in 100 μL optimized medium. The total number of cells used in the different experiments was determined by the trypan blue exclusion test (0.4%) using a cell counter. Cells were incubated for 24 hours before being treated with polymeric dispersions at concentrations ranging from 5.00 to 0.16 mg mL^{-1}. Treated cells were allowed to grow further for 48 hours. At the end of the incubation period, 20 μL of Cell Titer 96® AQ$_{ueous}$ One Solution Reagent (Promega-G3582) was added into each well and allowed to incubate at 37 °C for 2 hours in a humidified, 5% (v/v) CO_2 atmosphere. To measure the amount of soluble formazan produced by cellular reduction of 3-(4,5-dimethylthiazol-2-yl)-5-(3-carboxymethoxyphenyl)-2-(4-sulfophenyl)-2*H*-tetrazolium (MTS), the absorbance at 490 nm was recorded using Molecular Devices SectraMax Plus 384 Microplate Reader. Values of optical densities were normalized according to the negative control (untreated cells). Therefore, cell viability values of untreated cells were arbitrarily referred to

as 100% viability. Data are reported as mean ± standard deviation of three independent experiments.

Cellular uptake

Rhodamine B encapsulated vesicles were prepared in order to study the cellular uptake. Initially, HCT116 cells were grown into 96 wells plate at in 100 μL optimized medium in the same way as described above. The cells were then incubated with 0.63 mg mL^{-1} of Rhodamine B encapsulated vesicles at 37 °C for 2 hours and stained with Hoechst Stain Solution (H6024). Imaging of Hoechst-stained cells was performed using a confocal laser scanning microscope (CLSM: Zeiss Imager Z2 microscope equipped with LSM 780 CLSM and operated *via* Zeiss Zen 2012 software [Zeiss, Jena, Germany]). Hoechst fluorescence was excited at 405 nm, and emission was collected in the blue channel (~460–480 nm). Rhodamine fluorescence was excited at 561 nm, and emission was collected between 570–620 nm. Imaging was conducted using both a 63× water-immersion objective (Zeiss Objective C-Apochromat 63×/1.15 W Corr M27, FWD = 0.22 mm) for high-resolution imaging and a 20× objective (Zeiss Objective EC Plan-Neofluar 20×/0.5, WD = 2.0 mm) for overview scans. To avoid spectral overlap, each fluorophore was imaged separately to confirm the absence of cross-bleed between channels. Mean fluorescence intensity was obtained using the ImageJ (NIH) distribution Fiji. All CLSM imaging experiments were performed in triplicate to ensure reproducibility of the results.

Results and discussion

Synthesis of the PDMA macro-CTA precursor by RAFT polymerization

Herein, we report the first demonstration of PDPA-based vesicles prepared *via* RAFT-mediated PISA for the controlled delivery of 5-FU. To achieve this, poly(*N*,*N*-dimethylacrylamide) (PDMA) macro-chain transfer agent (macro-CTA) with a targeted degree of polymerization (DP) of 50 was initially synthesized by RAFT solution polymerization of (*N*,*N*-dimethylacrylamide) (DMA) with 4-4′-azobis(4-cyanovaleric acid) (ACVA) as the initiator at 60 °C and using 2-(dodecylthiocarbonothioylthio)2-methylpropanoic acid (DDMAT) as CTA (Scheme 1). The RAFT approach was particularly employed to provide control over the molecular weight and end group functionality.[15–17,43,44] The ratio of DDMAT to ACVA was kept low [1 : 0.2] to minimize termination and increase the fidelity of end groups required for subsequent PISA polymerization.

The monomer conversion was calculated using ^{1}H NMR of the crude reaction mixture before purification by using the integration of the PDMA methyl protons signal at 2.75 ppm and the integration of the vinyl DMA monomer proton signal at 6.44 ppm. A high monomer conversion of approximately 98% was achieved within 2.5 hours. Despite high monomer conversion achieved, high end group fidelity was maintained of 99% as estimated based on the integral value of DDMAT methyl end-group proton signal (i, CH_3CH_2–) at 0.88 ppm and the integral value of PDMA methyl group proton signal (d, –$N(CH_3)_2$) at 2.92 ppm (Fig. 2a).

The number average molecular weight (M_n) and dispersity ($Đ$) of PDMA macro-CTA were estimated using size exclusion chromatography (SEC), calibrated with near-monodisperse poly(methyl methacrylate) PMMA standards, and using DMF as eluent (Fig. 3a). M_n value of macro-CTA was 5100 g mol^{-1}, which is in a good agreement with theoretical M_n ($M_{n,theo}$) of 5250 g mol^{-1} calculated considering eqn (3).

$$M_{n,theo} = (DP \times MW_{DMA} \times conversion) + MW_{DDMAT} \quad (3)$$

However, the dispersity ($Đ$) value was 1.33, which is slightly higher than expected for a well-controlled RAFT polymerization. To investigate whether the high $Đ$ was real or merely a SEC artifact, the sample was further characterized using matrix-assisted laser desorption ionization-time of flight (MALDI-TOF) with linear mode and m/z upper limit of 20 kg mol^{-1}. The M_n obtained from MALDI-TOF was also 5100 g mol^{-1} (Fig. S1), consistent with SEC results. Importantly, the $Đ$ value obtained from MALDI-TOF was 1.02, confirming that the polymerization was indeed well-controlled and that the higher $Đ$ observed by SEC was likely due to calibration or separation artifacts.

Synthesis of PDMA50-*b*-PDPA$_m$ diblock copolymer vesicles *via* PISA

PISA dispersion polymerization was then used to synthesize the amphiphilic diblock copolymer, using water-soluble PDMA macro-CTA as the stabilizer, in the presence of ACVA as the initiator, at a fixed concentration of 20 wt% water : ethanol (4 : 6), under a nitrogen atmosphere. The use of this mixed solvent

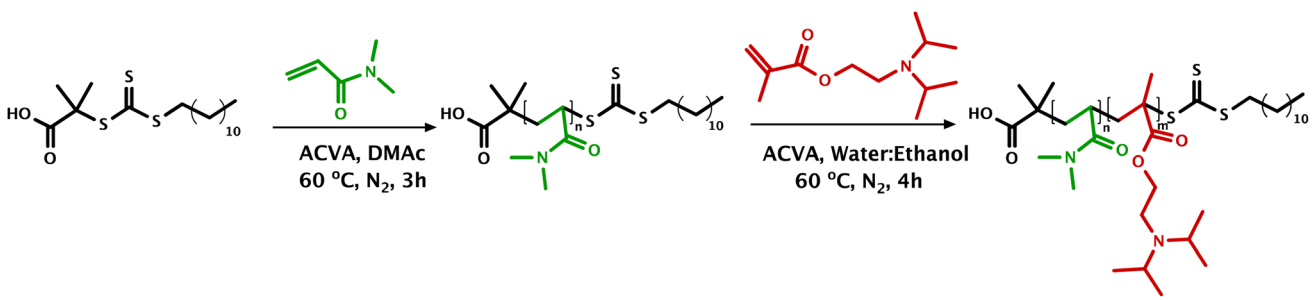

Scheme 1 Synthesis of pH-responsive PDMA$_{50}$-*co*-PDPA$_m$ diblock copolymer *via* RAFT PISA dispersion polymerization.

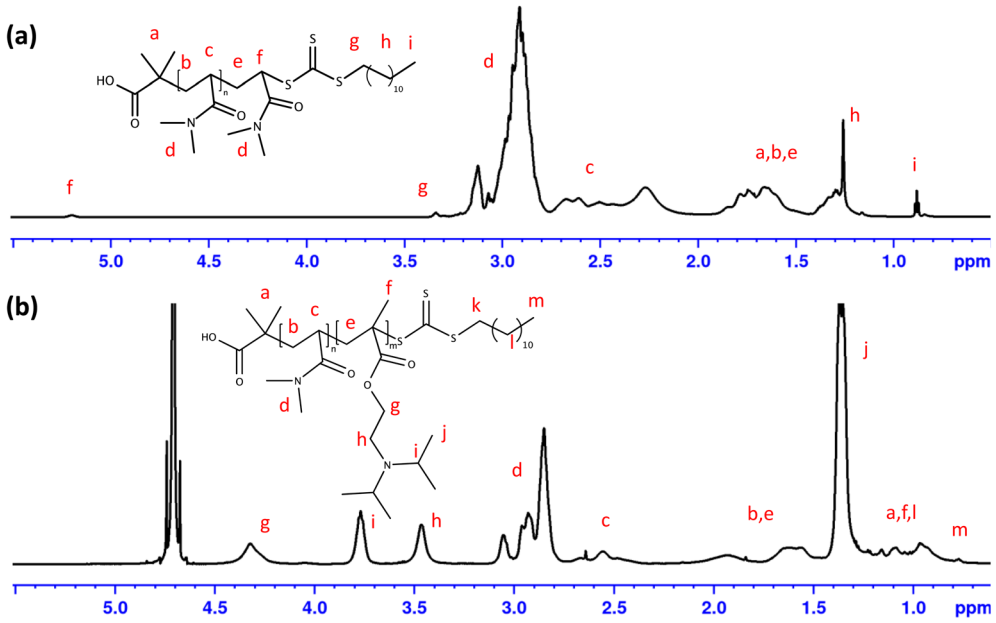

Fig. 2 ^{1}H NMR spectra of (a) PDMA macro-CTA in $CDCl_3$ and (b) $PDMA_{50}$-*b*-$PDPA_m$ in D_2O with trace amount of HCl.

allows the polymerization to proceed under dispersion conditions, which can give access to a wider range of morphologies.[45] The selected water : ethanol ratio provides an optimal balance between monomer solubility and particle nucleation. DPA is immiscible in water but readily soluble in ethanol; thus, ethanol maintains homogeneous reaction conditions during the early stages of polymerization, while water promotes micellar nucleation and faster particle growth once the core-forming block reaches its critical degree of polymerization. $PDMA_{50}$-*b*-$PDPA_m$ diblock copolymers with targeted DP of PDPA block of 150 and 200 were specially synthesized as these DPs should form pure vesicles according to phase diagram reported Zhang *et al.* for PISA alcoholic dispersion polymerization of PDPA core-building block.[26]

The successful synthesis of $PDMA_{50}$-*b*-$PDPA_m$ block copolymer was confirmed using ^{1}H NMR in D_2O (with a trace of HCl to solubilize PDPA block) with peaks observed at 4.32 ppm (g, –OCH_2CH_2–), 3.77 ppm (i, –$(CH\text{-}N)_2$–), 3.47 ppm (h, –CH_2CH_2N–), 1.50-2.05 ppm (e, –CH_2– of the polymer backbone), 1.36 ppm (j, –$(CH(CH_3)_2$–)), 0.95 ppm (f, "methacrylate" CH_3) assigned to PDPA block, along with other resonances corresponding to PDMA block and DDMAT end group (Fig. 2b).

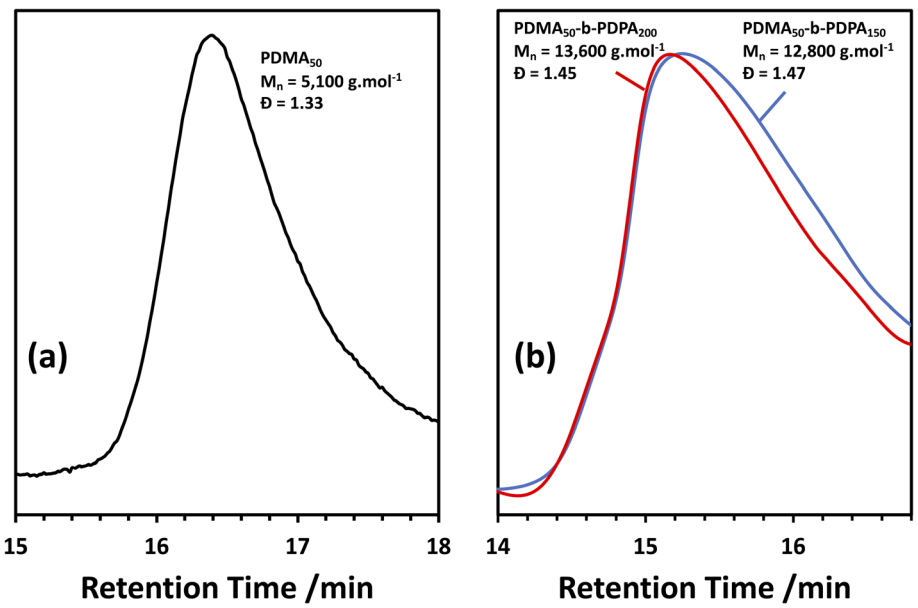

Fig. 3 (a) DMF SEC trace of PDMA macro-CTA calibrated using near-monodispersed PMMA standards. (b) THF SEC traces of $PDMA_{50}$-*b*-$PDPA_m$ block copolymers calibrated using near-monodisperse PMMA standards.

Table 1 Characterizations of the $PDMA_{50}$-*b*-$PDPA_m$ block copolymer synthesized *via* RAFT PISA

	Conv.[a] (%)	DP_{Actual}[a]	M_{nNMR}[b] (g mol^{-1})	M_{nSEC}[c] (g mol^{-1})	$Đ$[c]	Dz[d]	PI[d]
$PDMA_{50}$-*b*-$PDPA_{150}$	80%	120	30 850	12 800	1.47	305.1	0.11
$PDMA_{50}$-*b*-$PDPA_{200}$	69%	138	34 700	13 600	1.45	273.4	0.11

[a] Determined by ^{1}H NMR. [b] Calculated using eqn (4). [c] Determined by SEC using THF as eluent and PMMa calibration standards. [d] Determined *via* DLS after dilution with distilled water to 0.20 wt% at 25 °C.

The general characteristics of $PDMA_{50}$-*b*-$PDPA_m$, where *m* is the targeted DP of PDPA block, are summarized in Table 1. For $PDMA_{50}$-*b*-$PDPA_{150}$ and $PDMA_{50}$-*b*-$PDPA_{200}$, monomer conversions of 80% and 69%, respectively, were achieved within 4 hours, as determined by ^{1}H NMR spectroscopy of the crude reaction mixture prior to purification. The conversion was calculated by comparing the integration of the PDPA methyl proton signal at 1.36 ppm with that of the vinyl protons of unreacted DPA monomer at 5.67 ppm. The actual DPs of PDPA block was estimated using ^{1}H NMR of purified samples to be 120 and 138 for $PDPA_{150}$ and $PDPA_{200}$ targets, respectively. These were estimated by comparing the integrations of the signals corresponding to the methyl groups of PDMA (d,–$N(CH_3)_2$, δ = 2.92 ppm) and the methyl groups of PDPA (j, –$(CH(CH_3)_2$–), δ = 1.36 ppm) (Fig. 2b). Based on the actual DP values, $M_{n,NMR}$ were calculated to be 30 850 g mol^{-1} and 34 700 g mol^{-1}, considering eqn (4).

$$M_n = (DP_{Actual} \times MW_{DPA}) + M_{n,macro\text{-}CTA} \quad (4)$$

THF SEC, calibrated with a series of near-monodisperse PMMA standards, confirmed successful chain extension of the PDMA macro-CTA (Fig. 3b). The apparent M_n increased from 5250 g mol^{-1} for PDMA macro-CTA to 12 800 g mol^{-1} and 13 600 g mol^{-1} for $PDMA_{50}$-*b*-$PDPA_{150}$ and $PDMA_{50}$-*b*-$PDPA_{200}$, respectively, indicating efficient block copolymer formation. However, the $M_{n,SEC}$ values were markedly lower than those calculated from ^{1}H NMR analysis. This is due to the SEC analysis, which was calibrated against PMMA standards, which differ in hydrodynamic volume and chain conformation from the amphiphilic $PDMA_{50}$-*b*-$PDPA_m$ copolymers, resulting in an underestimated M_n. Moreover, The SEC traces were relatively broad ($Đ \approx$ 1.45–1.47), consistent with previous reports for PDPA-containing systems at high target DP values.[23]

The hydrophilic-to-hydrophobic ratio of the diblock copolymers, along with the total solid concentration, plays a critical role in the final morphology and the sizes of the self-assembled nanoparticles. The morphology of the self-assembled block copolymer nanoparticles might be qualitatively predicted by packing parameter (*P*), defined as

$$P = \frac{V}{a_0 l_c} \quad (5)$$

in which *V* and l_c are the volume and length of the hydrophobic block, and a_0 is the optimal interfacial area of the hydrophilic block. While spherical and worm-like particles are expected when $P > 1/2$, vesicles are likely to be formed when $1/2 < p < 1$.

The morphology of $PDMA_{50}$-*b*-$PDPA_m$ synthesized by PISA was characterized by TEM without staining. As illustrated in Fig. 4, both $PDMA_{50}$-*b*-$PDPA_{150}$ and $PDMA_{50}$-*b*-$PDPA_{200}$ display well-defined vesicle morphology, despite the relatively broad molecular weight distribution of the diblock copolymer ($Đ$ = 1.45). Previous PISA studies have shown that narrower dispersities promote more uniform self-assembly and pure phases,[46] while broader molecular weight distributions can induce packing heterogeneities, leading to mixed morphologies.[47]

The intensity-average diameter of the vesicles was determined *via* DLS after dilution with distilled water to 0.20 wt% at 25 °C. The vesicles exhibited relatively narrow particle size distributions (PI = 0.11), with intensity-average diameters ranging from 273 to 305 nm. A monotonic increase in particle size was observed with increasing the length (*i.e.*, DP) of PDPA, which is typical for PISA formulations and reflects the increased

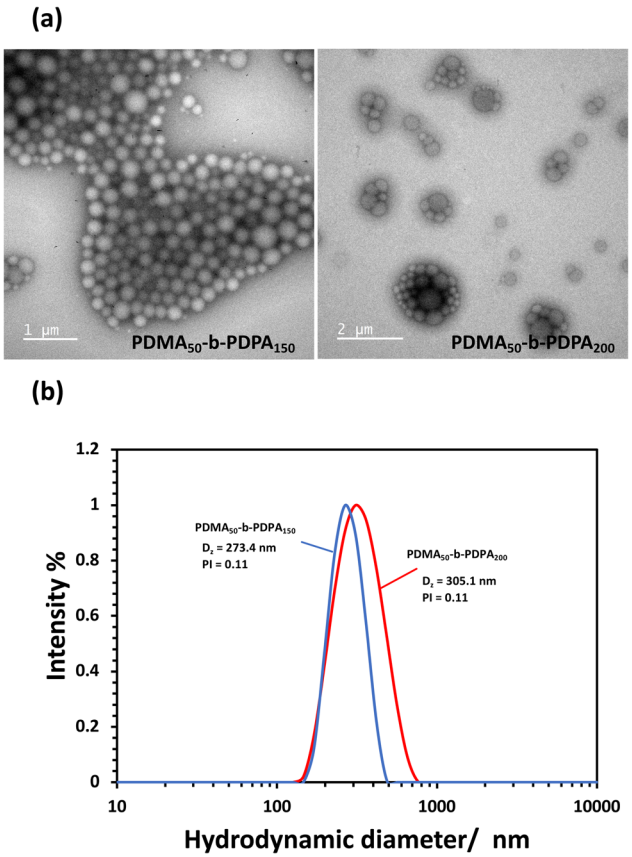

Fig. 4 (a) TEM images of $PDMA_{50}$-*b*-$PDPA_m$ in physiological pH (b) normalized DLS intensity-average particle size distributions recorded at 25 °C for 0.2% wt.

hydrophobic volume contributing to larger packing parameters and vesicle diameters.

pH-Response of the vesicles

Since the aim of this contribution is the investigation of the eligibility of the use of pH-responsive vesicles as 5-FU carriers, this section mainly focuses on $PDMA_{50}$-*b*-$PDPA_{200}$ assembly–disassembly transition in response to pH. Owing to the presence of a tertiary amino group in the PDPA block, the synthesized vesicles possess the capability to undergo a reversible deprotonation-protonation switch in response to an external pH. Under neutral conditions, the PDPA block is deprotonated and hydrophobic, forming stable vesicles. In contrast, at low pH, it is protonated and hydrophilic, leading to vesicle disassembly into soluble polymeric chains (unimers). This transition was visually evident, as the vesicle solution changed from turbid at pH 7.4 to transparent at pH 4.5 (Fig. 5a).

To characterize this pH-triggered behavior, the vesicle dispersions were diluted to a concentration of 0.2 wt% in either 0.1 M phosphate or acetate buffers for DLS and ζ-potential measurements as a function of pH (Fig. 5b). At pH > 5.5, the vesicles displayed a hydrodynamic diameter of approximately 350 nm and ζ-potential values around −40 mV, confirming the presence of stable, negatively charged vesicles possessing deprotonated terminal groups (Fig. 1b). Upon reducing the pH value below 5.5, a continuous decrease in the diameter was observed, accompanied by a sharp increase in the ζ-potential of around +30 mV. These changes indicate the protonation of the PDPA tertiary amines, resulting in a loss of hydrophobicity and vesicle disassembly into small aggregates. The observed

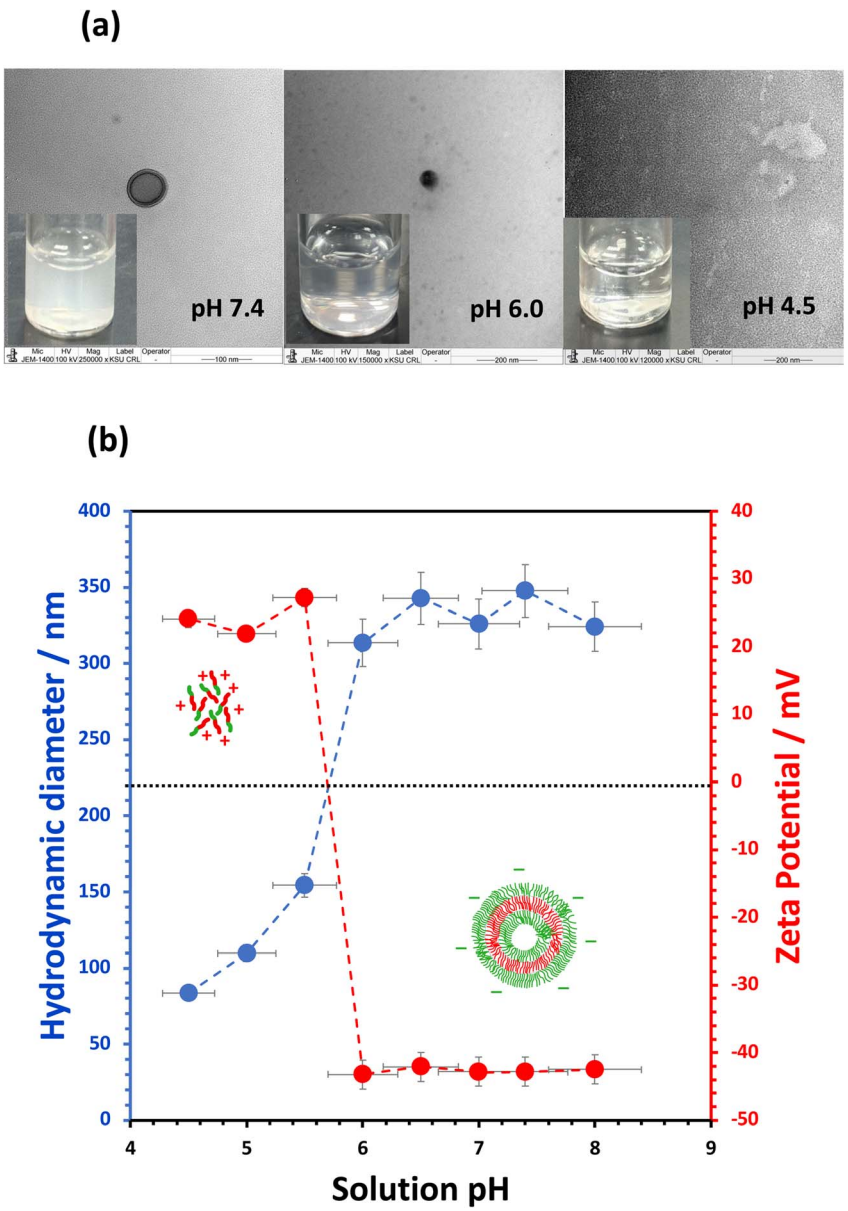

Fig. 5 (a) Disassembly of $PDMA_{50}$-*b*-$PDPA_{200}$ vesicle in response to pH (b) zeta potential *vs.* solution pH and hydrodynamic diameter *vs.* solution pH curves for a 0.2% w/w dispersion of $PDMA_{50}$-*b*-$PDPA_{200}$ copolymer at 25°.

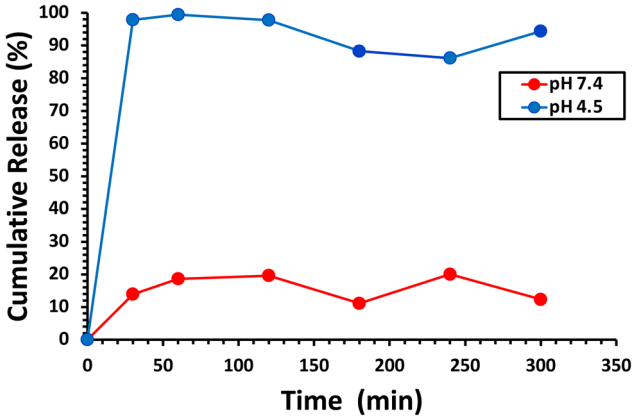

Fig. 6 Cumulative release profiles of 5-FU from $PDMA_{50}$-*b*-$PDPA_{200}$ loaded vesicles at pH 7.4 and pH 4.5.

transition pH (≈5.5) is slightly lower than the reported pK_a of PDPA (~6.3), which can be attributed to local environmental effects within the vesicle membrane and the presence of hydrophilic PDMA chains that might influence proton accessibility.

To investigate whether vesicle disassembly resulted in small polymer aggregates or was an artifact of DLS, TEM was utilized to further examine the morphology transition process. As illustrated in Fig. 5a, at pH 6.0, the internal structure was no longer visible, and the particle boundaries appeared diffuse, indicating the initial disassembly of the vesicles. At pH 4.5, no vesicle structures were detected, supporting complete morphological disassembly to unimer.

Cumulative release of 5-FU

Karagoz *et al.* and Armes group are perhaps the pioneers for *in situ* PISA encapsulation of various cargo molecules.[48,49] Despite the diversity of suitable cargo molecules, the *in situ* PISA encapsulation process has almost focused on small hydrophobic drugs/dyes.[50] While the process seems straightforward, *in situ* encapsulation often yields low cargo loading. Furthermore, recent reports found that cargo molecules might affect polymerization kinetics and morphology transitions.[51,52] For example, Cao *et al.* reported that *in situ* encapsulation of a hydrophobic drug facilitates morphology transition during the PISA process.[52]

In this manuscript, we report the encapsulation ability of 5-FU within pH responsive vesicles. 5-FU is a water-soluble drug and most likely to be encapsulated within the aqueous core (lumen) of the vesicle. Initial attempts for straightforward *in situ* encapsulation of 5-FU within the PISA process with targeted drug contents of 3.81, 1.90, and 0.95% failed to form particles. Hydrophilic 5-FU might delay nucleation and hence morphology transition. Therefore, the encapsulation ability of 5-FU into synthesized $PDMA_{50}$-*b*-$PDPA_{200}$ was evaluated using a passive post-PISA loading approach. After the removal of unencapsulated 5-FU *via* dialysis, the drug loading efficiency (LE) was estimated to be 30% for a targeted drug content of 3.81%. The obtained drug loading content (LC) was calculated to be 1.14%. The release of 5-FU was studied using two different media, namely phosphate buffer (pH 7.4, 0.1 M) and citrate buffer solution (pH 4.5, 0.1 M) simulating physiological pH and endosomal pH, respectively. The cumulative release of 5-FU over time is illustrated in Fig. 6. At pH 7.4, almost 15% of 5-FU was released within the first 30 min (burst release), which is probably the amount released from 5-FU-loaded polymeric vesicle suspension during storage. Burst release is a well-known phenomenon often reported for water-soluble, low-molecular-weight payloads.[53] After that, no significant release of 5-FU was observed within 300 min. This result demonstrates the capability of using pH-responsive vesicles to efficiently deliver a 5-FU payload to the tumor site, without significant release of 5-FU at physiological pH 7.4, and thus minimizing the side effects of 5-FU. In contrast, significant acceleration in 5-FU release was observed at pH 4.5. Nearly complete release of 5-FU was achieved within the first 30 minutes. The protonation of the tertiary amine of the PDPA block at low pH led to the disassembly of the vesicles and hence the rapid release of 5-FU.

Cytotoxicity and cellular uptake studies

Next, the cytotoxicity of the 5-FU-loaded $PDMA_{50}$-*b*-$PDPA_{200}$ vesicles was evaluated in HCT116 human colon cancer cells

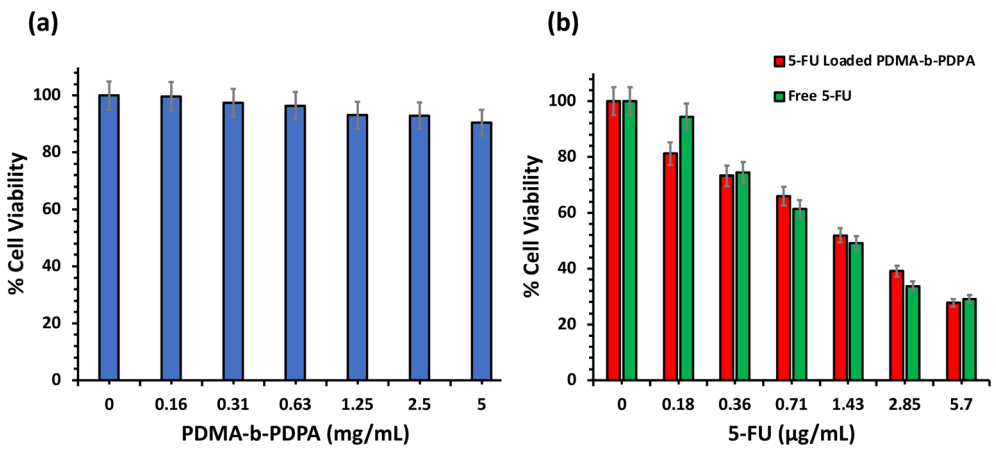

Fig. 7 Cytotoxicity MTS assay of (a) blank $PDMA_{50}$-*b*-$PDPA_{200}$, (b) 5-FU-loaded $PDMA_{50}$-*b*-$PDPA_{200}$ and free 5-FU in colon cell lines (HCT116) after 48 h incubation. The relative viability is expressed as percentage to control cells (untreated cell sample). Cytotoxicity experiments were performed in triplicate. Data are presented as mean ± standard deviation.

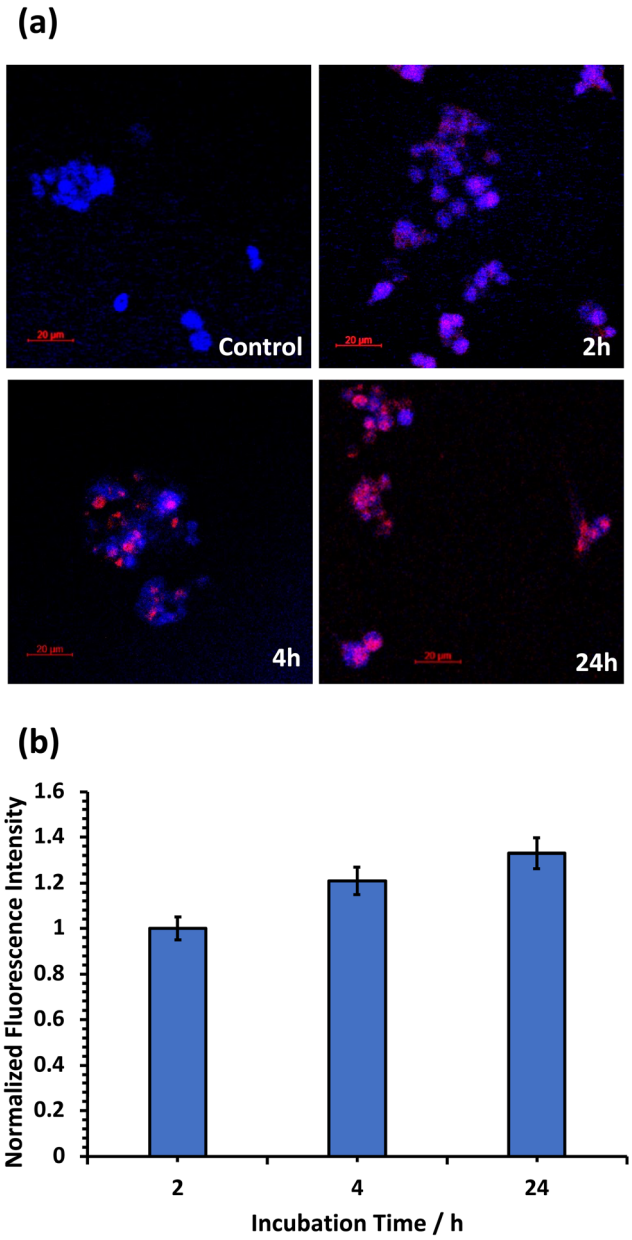

Fig. 8 (a) CLSM images of HCT116 cell lines incubated with 063 mg mL^{-1} Rhodamine B-loaded-$PDMA_{50}$-*b*-$PDPA_{200}$ vesicles at different incubation times. The cell nuclei were stained using Hoechst fluorescent dye. CLSM uptake experiments were performed in triplicate. (b) Normalized fluorescence intensity per cell for Rhodamine B-loaded vesicles uptake at different time points. Data was derived from CLSM images.

using an MTS assay. Cells were treated for 48 hours with different concentrations of either blank $PDMA_{50}$-*b*-$PDPA_{200}$ vesicles (0.16 to 5.00 mg mL^{-1}), 5-FU-loaded vesicles (corresponding to 0.18 to 5.70 μg mL^{-1} 5-FU), or free 5-FU at equivalent drug doses. The relative cell viabilities were compared to the control sample, which is arbitrarily referred to be 100%. As demonstrated in Fig. 7, the blank vesicles exhibited minimal cytotoxicity, maintaining >90% cell viability even at the highest concentration, consistent with previous reports on the biocompatibility of PDPA-based systems.[35]

In contrast, both free 5-FU and 5-FU-loaded vesicles induced dose-dependent cytotoxicity, with approximately 70% cell death observed at the highest dose (5.70 μg mL^{-1}). The comparable cytotoxicity profiles observed for free 5-FU and 5-FU-loaded vesicles, as determined by the MTS assay, indicate that the vesicular formulation effectively delivers 5-FU to the cells. This outcome suggests successful cellular internalization of the vesicles, followed by their disassembly and subsequent release of 5-FU within the acidic intracellular environment.

The cellular uptake of pH-responsive $PDMA_{50}$-*b*-$PDPA_{200}$ vesicles was then investigated in HCT116 cell line by encapsulating Rhodamine B, a hydrophilic red fluorescent dye, within the vesicles' aqueous core. This allowed tracking of the vesicles using confocal laser scanning microscopy (CLSM). Cell nuclei were stained with Hoechst 33342 to facilitate nuclear visualization. Cells incubated with vesicles were washed three times with PBS prior to imaging using CLSM to remove unbound free dye/vesicles from the extracellular space. No significant fluorescence signal was detected from the control sample incubated with free Rhodamine B, indicating that Rhodamine B has a limited capability to internalize into the cells *via* diffusion. This was consistent with previously reported studies using different cell lines.[35,54] In contrast, the Rhodamine B-loaded vesicles were efficiently internalized by the cells within two hours, and the fluorescence signal intensity became more pronounced with increasing incubation time to 24 h (Fig. 8). Moreover, CLSM images clearly revealed nuclear accumulation of Rhodamine B. This observation strongly suggests that cellular uptake occurred primarily through an endocytic mechanism, a common uptake mechanism for nanoscale systems. Upon internalization *via* endocytosis, the vesicles are trafficked into endo/lysosomal compartments, where the acidic pH induces disassembly of the PDPA core, facilitating intracellular release of Rhodamine B. The released dye is then able to diffuse into the nucleus, as evidenced by the localized fluorescence signal.

Taken together, the cytotoxicity and CLSM data confirm that the vesicles exhibit functional pH-responsiveness, highlighting their potential as smart nanocarriers for targeted delivery of 5-FU.

Conclusion

In this study, we successfully developed pH-responsive polymeric vesicles for the controlled delivery of 5-FU *via* PISA-mediated RAFT polymerization of DPA using a PDMA macro-CTA under aqueous dispersion conditions. The vesicles underwent rapid disassembly under endosomal pH, as confirmed by TEM, DLS, and ζ-potential analyses. This pH-triggered structural transition enabled the selective release of 5-FU in acidic environments, leading to efficient intracellular delivery. Cytotoxicity and CLSM studies further demonstrated that the vesicles were biocompatible in their blank form, while 5-FU-loaded vesicles achieved therapeutic efficacy comparable to that of the free drug, with effective cellular uptake and nuclear localization in HCT116 cells.

To the best of our knowledge, this represents the first example of PDPA-containing block copolymer vesicles used for

5-FU delivery. Overall, this work highlights a versatile and straightforward strategy to engineer pH-responsive vesicles with potential for targeted and stimuli-responsive cancer therapy. Beyond 5-FU, this platform could be adapted for the delivery of other hydrophilic therapeutics, paving the way for future applications in smart nanomedicine.

Conflicts of interest

The authors declare no conflict of interest.

Data availability

All the data supporting the findings of this study, including MALDI-TOF, DLS measurements, and UV calibration data, are available in the supplementary information (SI). Supplementary information is available. See DOI: https://doi.org/10.1039/d5ra06313b.

Acknowledgements

The authors extend their appreciation to the Deanship of Postgraduate Studies and Scientific Research at Majmaah University for funding this research work through the project number R-2025-2174. This project was funded by the Research Institute/Center Supporting Program (RICSP-25-3), King Saud University, Riyadh, Saudi Arabia. The authors would also like to thank the King Abdullah University for Science and Technology Core Labs, KAUST, Thuwal, Saudi Arabia, for their assistance with SEC, TEM, and NMR analysis.

References

1 J. Rodríguez-Hernández, F. Chécot, Y. Gnanou and S. Lecommandoux, Toward 'smart' nano-objects by self-assembly of block copolymers in solution, *Prog. Polym. Sci.*, 2005, **30**, 691–724.
2 Y. Mai and A. Eisenberg, Self-assembly of block copolymers, *Chem. Soc. Rev.*, 2012, **41**, 5969–5985.
3 J. Wang, M. Cao, P. Zhou and G. Wang, Exploration of a Living Anionic Polymerization Mechanism into Polymerization-Induced Self-Assembly and Site-Specific Stabilization of the Formed Nano-Objects, *Macromolecules*, 2020, **53**, 3157–3165.
4 C. Zhou, J. Wang, P. Zhou and G. Wang, A polymerization-induced self-assembly process for all-styrenic nano-objects using the living anionic polymerization mechanism, *Polym. Chem.*, 2020, **11**, 2635–2639.
5 G. Wang, M. Schmitt, Z. Wang, B. Lee, X. Pan, L. Fu, J. Yan, S. Li, G. Xie, M. R. Bockstaller and K. Matyjaszewski, Polymerization-induced self-assembly (PISA) using ICAR ATRP at low catalyst concentration, *Macromolecules*, 2016, **49**, 8605–8615.
6 A. Alzahrani, D. Zhou, R. P. Kuchel, P. B. Zetterlund and F. Aldabbagh, Polymerization-induced self-assembly based on ATRP in supercritical carbon dioxide, *Polym. Chem.*, 2019, **10**, 2658–2665.
7 G. Delaittre, C. Dire, J. Rieger, J. L. Putaux and B. Charleux, Formation of polymer vesicles by simultaneous chain growth and self-assembly of amphiphilic block copolymers, *Chem. Commun.*, 2009, 2887–2889.
8 C. J. Ferguson, R. J. Hughes, B. T. T. Pham, B. S. Hawkett, R. G. Gilbert, A. K. Serelis and C. H. Such, Effective ab Initio Emulsion Polymerization under RAFT Control, *Macromolecules*, 2002, **35**, 9243–9245.
9 Y. Li and S. P. Armes, RAFT Synthesis of sterically stabilized methacrylic nanolatexes and vesicles by aqueous dispersion polymerization, *Angew. Chem., Int. Ed.*, 2010, **49**, 4042–4046.
10 S. L. Canning, G. N. Smith and S. P. Armes, A Critical Appraisal of RAFT-Mediated Polymerization-Induced Self-Assembly, *Macromolecules*, 2016, **49**, 1985–2001.
11 N. J. W. Penfold, J. Yeow, C. Boyer and S. P. Armes, Emerging Trends in Polymerization-Induced Self-Assembly, *ACS Macro Lett.*, 2019, **8**, 1029–1054.
12 J. Wan, B. Fan and S. H. Thang, RAFT-mediated polymerization-induced self-assembly (RAFT-PISA): current status and future directions, *Chem. Sci.*, 2022, **13**, 4192–4224.
13 E. J. Cornel, J. Jiang, S. Chen and J. Du, Principles and characteristics of polymerization-induced self-assembly with various polymerization techniques, *CCS Chem.*, 2021, **3**, 2104–2125.
14 C. György and S. P. Armes, Recent Advances in Polymerization-Induced Self-Assembly (PISA) Syntheses in Non-Polar Media, *Angew. Chem., Int. Ed.*, 2023, **62**, e202308372.
15 J. Chiefari, Y. K. Chong, F. Ercole, J. Krstina, J. Jeffery, T. P. T. Le, R. T. A. Mayadunne, G. F. Meijs, C. L. Moad, G. Moad, E. Rizzardo and S. H. Thang, Living free-radical polymerization by reversible addition - Fragmentation chain transfer: The RAFT process, *Macromolecules*, 1998, **31**, 5559–5562.
16 S. Perrier, 50th Anniversary Perspective: RAFT Polymerization - A User Guide, *Macromolecules*, 2017, **50**, 7433–7447.
17 M. R. Hill, R. N. Carmean and B. S. Sumerlin, Expanding the Scope of RAFT Polymerization: Recent Advances and New Horizons, *Macromolecules*, 2015, **48**, 5459–5469.
18 B. M. Discher, Y. Y. Won, D. S. Ege, J. C. M. Lee, F. S. Bates, D. E. Discher and D. A. Hammer, Polymersomes: Tough vesicles made from diblock copolymers, *Science*, 1999, **284**, 1143–1146.
19 R. P. Brinkhuis, F. P. J. T. Rutjes and J. C. M. Van Hest, Polymeric vesicles in biomedical applications, *Polym. Chem.*, 2011, **2**, 1449–1462.
20 T. Thambi, V. G. Deepagan, H. Ko, D. S. Lee and J. H. Park, Bioreducible polymersomes for intracellular dual-drug delivery, *J. Mater. Chem.*, 2012, **22**, 22028–22036.
21 Y. Pei, A. B. Lowe and P. J. Roth, Stimulus-Responsive Nanoparticles and Associated (Reversible) Polymorphism via Polymerization Induced Self-assembly (PISA), *Macromol. Rapid Commun.*, 2017, **38**, 1–14.
22 X. Hu, Y. Zhang, Z. Xie, X. Jing, A. Bellotti and Z. Gu, Stimuli-Responsive Polymersomes for Biomedical Applications, *Biomacromolecules*, 2017, **18**, 649–673.

23 C. J. Mable, L. A. Fielding, M. J. Derry, O. O. Mykhaylyk, P. Chambon and S. P. Armes, Synthesis and pH-responsive dissociation of framboidal ABC triblock copolymer vesicles in aqueous solution, *Chem. Sci.*, 2018, **9**, 1454–1463.

24 M. Chen, J. W. Li, W. J. Zhang, C. Y. Hong and C. Y. Pan, PH- and Reductant-Responsive Polymeric Vesicles with Robust Membrane-Cross-Linked Structures: In Situ Cross-Linking in Polymerization-Induced Self-Assembly, *Macromolecules*, 2019, **52**, 1140–1149.

25 S. Lukáš Petrova, V. Sincari, R. Konefał, E. Pavlova, M. Hrubý, V. Pokorný and E. Jäger, Microwave Irradiation-Assisted Reversible Addition-Fragmentation Chain Transfer Polymerization-Induced Self-Assembly of pH-Responsive Diblock Copolymer Nanoparticles, *ACS Omega*, 2022, **7**, 42711–42722.

26 F. Zhang, Y. Niu, Y. Li, Q. Yao, X. Chen, H. Zhou, M. Zhou and J. Xiao, Fabrication and characterization of structurally stable pH-responsive polymeric vesicles by polymerization-induced self-assembly, *RSC Adv.*, 2021, **11**, 29042–29051.

27 T. Yildirim, A. Traeger, P. Sungur, S. Hoeppener, C. Kellner, I. Yildirim, D. Pretzel, S. Schubert and U. S. Schubert, Polymersomes with Endosomal pH-Induced Vesicle-to-Micelle Morphology Transition and a Potential Application for Controlled Doxorubicin Delivery, *Biomacromolecules*, 2017, **18**, 3280–3290.

28 C. A. Figg, A. Simula, K. A. Gebre, B. S. Tucker, D. M. Haddleton and B. S. Sumerlin, Polymerization-induced thermal self-assembly (PITSA), *Chem. Sci.*, 2015, **6**, 1230–1236.

29 A. Blanazs, R. Verber, O. O. Mykhaylyk, A. J. Ryan, J. Z. Heath, C. W. I. Douglas and S. P. Armes, Sterilizable gels from thermoresponsive block copolymer worms, *J. Am. Chem. Soc.*, 2012, **134**, 9741–9748.

30 B. Fan, J. Wan, J. Zhai, X. Chen and S. H. Thang, Triggered Degradable Colloidal Particles with Ordered Inverse Bicontinuous Cubic and Hexagonal Mesophases, *ACS Nano*, 2021, **15**, 4688–4698.

31 P. Shi, Y. Qu, C. Liu, H. Khan, P. Sun and W. Zhang, Redox-Responsive Multicompartment Vesicles of Ferrocene-Containing Triblock Terpolymer Exhibiting On-Off Switchable Pores, *ACS Macro Lett.*, 2016, **5**, 88–93.

32 W. Gao, J. M. Chan and O. C. Farokhzad, pH-Responsive Nanoparticles for Drug Delivery, *Mol. Pharm.*, 2010, **7**, 1913–1920.

33 A. Car, P. Baumann, J. T. Duskey, M. Chami, N. Bruns and W. Meier, PH-responsive PDMS-b-PDMAEMA micelles for intracellular anticancer drug delivery, *Biomacromolecules*, 2014, **15**, 3235–3245.

34 E. Jäger, P. Černoch, M. Vragovic, L. J. Calumby Albuquerque, V. Sincari, T. Heizer, A. Jäger, J. Kučka, O. Š. Janoušková, E. Pavlova, L. Šefc and F. C. Giacomelli, Membrane Permeability and Responsiveness Drive Performance: Linking Structural Features with the Antitumor Effectiveness of Doxorubicin-Loaded Stimuli-Triggered Polymersomes, *Biomacromolecules*, 2024, **25**, 4192–4202.

35 H. Lomas, M. Massignani, K. A. Abdullah, I. Canton, C. Lo Presti, S. MacNeil, J. Du, A. Blanazs, J. Madsen, S. P. Armes, A. L. Lewis and G. Battaglia, Non-cytotoxic polymer vesicles for rapid and efficient intracellular delivery, *Faraday Discuss.*, 2008, **139**, 143–159.

36 D. B. Longley, D. P. Harkin and P. G. Johnston, 5-Fluorouracil: Mechanisms of action and clinical strategies, *Nat. Rev. Cancer*, 2003, **3**, 330–338.

37 D. Putnam and J. Kopeček, Enantioselective Release of 5-Fluorouracil from N-(2-Hydroxypropyl)Methacrylamide-Based Copolymers via Lysosomal Enzymes, *Bioconjugate Chem.*, 1995, **6**, 483–492.

38 M. Nichifor, E. H. Schacht and L. W. Seymour, Macromolecular prodrugs of 5-fluorouracil. 2: Enzymatic degradation, *J. Controlled Release*, 1996, **39**, 79–92.

39 L. M. Alhaidari and S. G. Spain, Synthesis of 5-Fluorouracil Polymer Conjugate and 19F NMR Analysis of Drug Release for MRI Monitoring, *Polymers*, 2023, **15**, 1778.

40 A. M. Thomas, A. I. Kapanen, J. I. Hare, E. Ramsay, K. Edwards, G. Karlsson and M. B. Bally, Development of a liposomal nanoparticle formulation of 5-Fluorouracil for parenteral administration: Formulation design, pharmacokinetics and efficacy, *J. Controlled Release*, 2011, **150**, 212–219.

41 M. Fresta, A. Villari, G. Puglisi and G. Cavallaro, 5-Fluorouracil: various kinds of loaded liposomes: encapsulation efficiency, storage stability and fusogenic properties, *Int. J. Pharm.*, 1993, **99**, 145–156.

42 W. Khalid, K. U. Shah, M. D. Saeed, A. Nawaz, F. U. Rehman, M. Shoaib, M. U. Rehman, A. F. Alasmari, M. Alharbi and F. Alasmari, 5-Fluorouracil-Loaded Hyaluronic Acid-Coated Niosomal Vesicles: Fabrication and Ex Vivo Evaluation for Skin Drug Delivery, *ACS Omega*, 2023, **8**, 45405–45413.

43 R. T. A. Mayadunne, E. Rizzardo, J. Chiefari, Y. K. Chong, G. Moad and S. H. Thang, Living radical polymerization with reversible addition-fragmentation chain transfer (RAFT polymerization) using dithiocarbamates as chain transfer agents, *Macromolecules*, 1999, **32**, 6977–6980.

44 D. J. Keddie, A guide to the synthesis of block copolymers using reversible-addition fragmentation chain transfer (RAFT) polymerization, *Chem. Soc. Rev.*, 2014, **43**, 496–505.

45 C. Liu, C.-Y. Hong and P. Cai-Yuan, Polymerization Techniques in Polymerization-Induced Self- Assembly (PISA), *Polym. Chem.*, 2012, **11**, 3673–3689.

46 C. Q. Huang and C. Y. Pan, Direct preparation of vesicles from one-pot RAFT dispersion polymerization, *Polymer*, 2010, **51**, 5115–5121.

47 A. Blanazs, J. Madsen, G. Battaglia, A. J. Ryan and S. P. Armes, Mechanistic insights for block copolymer morphologies: How do worms form vesicles?, *J. Am. Chem. Soc.*, 2011, **133**, 16581–16587.

48 B. Karagoz, C. Boyer and T. P. Davis, Simultaneous polymerization-induced self-assembly (PISA) and guest molecule encapsulation, *Macromol. Rapid Commun.*, 2014, **35**, 417–421.

49 C. J. Mable, R. R. Gibson, S. Prevost, B. E. McKenzie, O. O. Mykhaylyk and S. P. Armes, Loading of Silica

Nanoparticles in Block Copolymer Vesicles during Polymerization-Induced Self-Assembly: Encapsulation Efficiency and Thermally Triggered Release, *J. Am. Chem. Soc.*, 2015, **137**, 16098–16108.

50 E. G. Hochreiner and B. G. P. van Ravensteijn, Polymerization-induced self-assembly for drug delivery: A critical appraisal, *J. Polym. Sci.*, 2023, **61**, 3186–3210.

51 F. H. Sobotta, M. T. Kuchenbrod, F. V. Gruschwitz, G. Festag, P. Bellstedt, S. Hoeppener and J. C. Brendel, Tuneable Time Delay in the Burst Release from Oxidation-Sensitive Polymersomes Made by PISA, *Angew. Chem., Int. Ed.*, 2021, **60**, 24716–24723.

52 C. Cao, F. Chen, C. J. Garvey and M. H. Stenzel, Drug-Directed Morphology Changes in Polymerization-Induced Self-Assembly (PISA) Influence the Biological Behavior of Nanoparticles, *ACS Appl. Mater. Interfaces*, 2020, **12**, 30221–30233.

53 X. Huang and C. S. Brazel, On the importance and mechanisms of burst release in matrix-controlled drug delivery systems, *J. Controlled Release*, 2001, **73**, 121–136.

54 R. Misra and S. K. Sahoo, Intracellular trafficking of nuclear localization signal conjugated nanoparticles for cancer therapy, *Eur. J. Pharm. Sci.*, 2010, **39**, 152–163.